On phase synchronization by periodic force in chaotic oscillators with saddle equilibria

Michael A. Zaks, Eun-Hyoung Park, Jürgen Kurths

Institute of Physics, Potsdam University,
PF 601553, D-14415 Potsdam Germany

Abstract

A periodic action onto a chaotic system can result in phase synchronization: although the oscillations remain chaotic, their pace is prescribed by the rhythm of the force. We show how this adjustment of characteristic timescales to the period of the forcing is violated when, due to the presence of a saddle point in the autonomous attractor, the time intervals between returns onto a Poincaré plane are unbounded. In such situation, the segments of a chaotic trajectory in which its phase follows the phase of the force, can alternate with short segments of phase-locking in ratios different from 1:1. This phenomenon is demonstrated for several nonlinear systems.

1 Introduction

Chaotic systems in the state of phase synchronization [Rosenblum *et al.*, 1996] occupy in nonlinear dynamics of coupled oscillators a place between the stage in which the coupling is too weak to invoke correlations between the subsystems, and the stage of "generalized synchronization" [Rulkov *et al.*, 1995, Kocarev & Parlitz, 1996] when all subsystems exhibit the same (up to the functional mapping) dynamical pattern[1]. Phase synchronization is understood as a particular kind of collective dynamics: chaotic oscillations in all subsystems follow the common pace but the other characteristics remain uncorrelated. In particular, perturbed by periodic external force chaotic oscillators, while remaining chaotic, are known to adapt their rhythm to the period of forcing [Rulkov, 1996, Pikovsky *et al.*, 1997c].

For a chaotic system with a narrow band of characteristic timescales, it appears to be not too difficult to adjust its dynamics to the action of the external factor whose period either belongs to this band or lies close to it; that is the way how phase synchronization manifests itself in the externally driven Rössler equations [Rosenblum *et al.*, 1996]. The situation is less transparent for chaotic systems whose typical timecales (expressed, e.g. through intervals between the returns onto an appropriate Poincaré surface) are scattered over a broad range, or are even unbounded; the latter happens when the chaotic attractor of an autonomous system includes an unstable state of equilibrium. Once reinjected into the neighborhood of such state, the system may require arbitrarily long to leave it. In this case the ideal phase synchronization when the phase of the driven chaotic oscillator follows the phase of the driving force, may prove unreachable; instead, a certain kind of imperfect phase synchronization [Zaks *et al.*, 1999] can

[1] The latter stage, in its turn, may prove to be a prelude to the "complete synchronization" [Fujisaka & Yamada, 1983, Pikovsky, 1984, Pecora & Carroll, 1990] in which the subsystems display identical dynamics.

be achieved, in which long time intervals when the phases follow each other, are interrupted by phase "jumps" during which one of the partners runs a cycle ahead.

In this paper, we further investigate the implications for phase synchronization caused by the presence of saddle-points in the autonomous attractors. We interpret the observed phenomena by visualizing the unstable periodic orbits embedded into the attractor. Unstable periodic orbits are omnipresent in chaotic dynamics [Cvitanović, 91]; knowledge of their features allows to characterize, both qualitatively and quantitatively, the properties of strange sets. In the context of phase synchronization the unstable periodic orbits were successfully employed in [Pikovsky *et al.*, 1997a] where their usage allowed, first, to delineate in the parameter space the domain of phase synchronization and, second, to characterize desynchronization as a certain kind of intermittency caused by the attractor-repeller collision (see also [Rosa *et al.*, 1998]).

Each periodic solution can be viewed as a separate oscillator; when a periodic force acts onto this oscillator, phase lockings can occur. According to [Pikovsky *et al.*, 1997a], perfect phase synchronization results from the overlap in the parameter space of the locking regions for all relevant unstable periodic orbits; the ratio of frequencies ("locking ratio") for all these orbits should be the same. This conjecture was confirmed for the periodically forced Rössler system [Pikovsky *et al.*, 1997b]. Imperfect phase synchronization, in its turn, has been shown to be caused by the overlap of the regions which correspond to different locking ratios. Presence of saddle points in the attractor of the autonomous system implies that infinitesimal perturbations of the system can form closed trajectories which tend to these saddle points at $t \to \pm\infty$: homoclinic orbits. Destruction of homoclinic orbits creates periodic trajectories with very long period and, hence, low frequencies, much lower than the frequencies of all the other periodic orbits belonging to the attractor. We intend to study the peculiarities of phase synchronization which occur when a periodic external force acts onto such system.

It is hardly possible to detect phase synchronization or its absence without computing the phase itself. Since the phase of a chaotic motion is not directly available from observations, we have to reconstruct it by indirect measurements. What we need, is some kind of registry for the events which are approximately repeated in the course of the chaotic process, and whose frequency measures the pace of dynamics; in terms of phase space they correspond to the returns onto some Poincaré surface. The approach of "analytic signal" introduced in [Gabor, 1946], decomposes the signal into the instantaneous amplitude and the instantaneous phase by means of the Hilbert transformation. In fact, knowledge of the phase *between* the returns is not very important; much more significant is the ability to compare over long time the amount of these returns with the number of periods of external forcing. Accordingly, below we will infer the phase by counting intersections of the orbit with the Poincaré surface. We will denote by the word "orbit turn" or "turn" a segment of orbit between two consecutive returns onto the prescribed surface and set that each orbit turn increases the value of the phase by 2π. "Inside" the turns (in fact, we hardly need these intermediate values of the phase) the running phase value can be estimated through linear interpolation [Pikovsky *et al.*, 1997c]: for $t_k < t < t_{k+1}$ where t_k and t_{k+1} denote the time moments of, respectively, the k-th and the $k+1$-th intersections with the Poincaré plane, the instantaneous value of the phase $\Phi(t)$ is given by

$$\Phi(t) = 2\pi k + 2\pi \frac{t - t_k}{t_{k+1} - t_k} \tag{1}$$

Accordingly, the mean frequency of the chaotic motion is defined as the growth rate of the phase and can be computed as

$$\omega = \lim_{N \to \infty} \frac{2\pi N}{t(N)} \tag{2}$$

where $t(N)$ denotes the amount of time required to complete N turns. Numerically, we have found that setting N to 10^6 allows to compute ω to the precision of 4-5 decimal digits and makes the (in general, necessary) averaging over many initial conditions on the attractor redundant: in all calculations below the frequency of chaotic motion was estimated from this value of N.

In order to characterize chaotic states in terms of embedded unstable periodic orbits, we need to introduce the corresponding vocabulary. The number of turns of the closed trajectory (i.e. the number of loops it makes in the phase space) is denoted as length of the periodic orbit [Pikovsky *et al.*, 1997b]; unlike the period of the orbit, this dimensionless topological characteristics is an integer number. Further, the individual frequency of the periodic orbit $\omega_{\rm i}$ is defined as the average frequency per one turn of the orbit: $\omega_{\rm i} = 2\pi l/T$ where l is the length of the orbit and T is its period.

When a weak periodic force acts onto an autonomous system with an unstable periodic solution, the unstable invariant torus replaces in the phase space the unstable closed curve. In our numerical studies we fix the internal parameters of the system, reducing the parameter space to the plane spanned by the frequency and the amplitude of the force. In accordance with the general theory of oscillations, synchronization occurs in the wedge-shaped regions (Arnold tongues) opening from the abscissa of this parameter plane. Inside these regions the frequencies of the force and of the motion are locked in rational ratios. Here, two periodic orbits exist on the torus: on its surface, one of them is stable; we call it "phase-stable" since the torus itself is unstable. The second periodic orbit is unstable ("phase-unstable"). On the borders of the Arnold tongues periodic orbits collide and disappear through the tangent bifurcation; outside the locking regions the motion on the torus is not synchronized. According to the conjecture of [Pikovsky *et al.*, 1997a], unstable tori may play in the phase space of the periodically forced chaotic system the role analogous to the role of unstable periodic orbits in the autonomous chaotic system: typical trajectories wander between them. When a chaotic trajectory passes close to a locked torus, it approaches the phase-stable solution and, during a certain time, it remains locked to the external force in the same frequency ratio as this solution; then the instability of the torus repels it to the next torus, and so on. Should all the tori be synchronized with the external force in the same locking ratio, chaotic orbits would obey this ratio too, exhibiting perfect phase synchronization. If some of the tori are not locked, the passage near them would violate phase locking, and chaotic orbit would display desynchronized dynamics (in the form of intermittency, if the proportion of such tori is small). Finally, if all the tori are locked but the locking ratios differ from one torus to another one, one should be able to visualize in the long chaotic trajectory the alternating segments corresponding to these different lockings: the epochs of imperfect phase synchronization.

For our examples, we use three ODE systems of the 3-rd order. In all cases we observe the onset of imperfect phase synchronization. In the forced Lorenz equations treated in Sect. 2, the homoclinic bifurcations, which should occur from a small perturbation in the autonomous equations, produce periodic orbits with large number of loops ("turns") in the phase space; these orbits do not seem to influence the mechanism of synchronization. We demonstrate that here the passage near the saddle point results, paradoxically, in the increase of the individual frequency for the relevant unstable periodic orbit, and explain how this leads to imperfect phase synchronization. A slightly different picture of imperfect phase synchronization is presented in Sect. 3; there we apply periodic force to the Shimizu-Morioka equations, whose parameter values are tuned in the way which puts the autonomous system close to the formation of short homoclinic orbits. We show how this proximity leads to the deformation of the Arnold tongues. Finally, in Sect. 4 we describe the synchronizing action of periodic forcing onto the temporal chaos which arises in the context of pattern formation in continuous media: a low-dimensional model of the weakly dissipative Ginzburg-Landau equation; here, also, the mechanism behind the onset of imperfect phase synchronization is the alternation of different locking ratios.

In our numerical investigations, we compute both the global and the "local" (associated to particular periodic orbits) characteristics. For the global dynamics on the attractor, we follow a chaotic trajectory until $N = 10^6$ intersections with the Poincaré surface and evaluate the mean frequency of the chaotic motion. For individual periodic orbits embedded into the attractor, we estimate the position of locking regions in the parameter space. A periodic orbit of length l is represented by the fixed point of the mapping induced on the Poncaré surface by l turns of the flow. To determine the boundary of the locking region, we numerically locate the parameter values under which one of the eigenvalues of the linearization of the latter mapping near the corresponding fixed point equals 1; in this procedure the Newton technique is combined with polynomial prediction in the parameter space.

2 Phase synchronization in the forced Lorenz equations

As our first example we consider the Lorenz equations [Lorenz, 1963]

$$\begin{aligned} \dot{x} &= \sigma(y-x), \\ \dot{y} &= rx - y - xz, \\ \dot{z} &= xy - bz + E\cos(\Omega t) \end{aligned} \tag{3}$$

perturbed by a periodic external force with amplitude E and frequency Ω. For our numerical analysis we use the standard parameter values $\sigma = 10$ and $b = 8/3$ from [Lorenz, 1963]. Regarding the third parameter r, we will mostly employ the value $r = 28$ from the original paper of Lorenz. Our description, however, begins with the brief demonstration of perfect phase synchronization in a periodically driven chaotic system, and the forced Lorenz model at $r = 210$ provides a clear and distinct illustration of phase synchronization which is *not* hindered by the presence of the saddle point in the autonomous chaotic attractor. For the computation of the phase, we use the Poincaré plane located at $z = r - 1$ and count the intersections at which $\dot{z}$ is negative.

2.1 Phase synchronization in a system with a narrow band of return times

At high values of r the autonomous Lorenz equations exhibit bifurcation scenarios which do not involve a saddle point ([Sparrow, 1982]. Under the value $r = 210$ the autonomous Eqs.(3) possess two symmetric chaotic attracting sets (Fig. 1a); the stable manifold of the saddle point at the origin $x = y = z = 0$ separates the basins of these attractors in the phase space, but the point itself does not belong to the attractor. The return time onto the Poincaré surface is confined to a narrow interval; the individual frequencies ω_i of unstable periodic orbits embedded in the attractor, are strongly localized: as seen in Fig. 1b, deviations from the mean value of ω_i do not exceed 0.2%.

Such an attractor easily yields to the synchronizing action of the external periodic force whose frequency is not too far from its own. Provided, the amplitude of the force is sufficiently large ($E > 0.5$ is enough), the difference between the driving frequency Ω and the mean frequency of the chaotic motion ω vanishes identically in a rather broad range of values of Ω (Fig. 2a).

The coincidence between Ω and ω, being a necessary condition for phase synchronization, is not sufficient: it would also hold if the phases of the force and the system diverge in such a way that the difference between them grows sublinearly in time. To ensure that the states

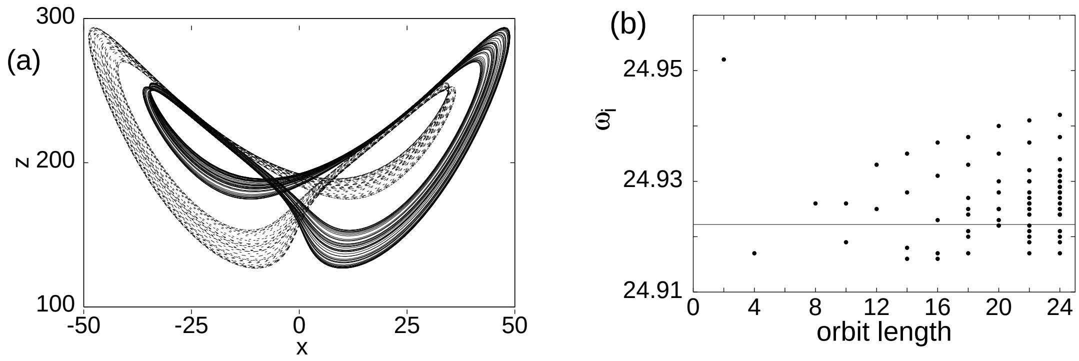

Figure 1: Autonomous Lorenz equations at r=210:
a) projection of two symmetric attractors;
b) individual frequencies of periodic orbits (dots); dashed line: mean frequency of the chaotic motion.

inside the plateau of Fig. 2a are phase-synchronized, we plot in Fig. 2b,c the coordinates of intersections with the Poincaré plane; here, Ψ is the value of the phase of the external force at the moment of intersection. Unlike the diffuse cloud which corresponds to the non-synchronized case (Fig. 2b), the attractor of the synchronized state (Fig. 2c) is localized with regard to the phase variable Ψ. Computation of the Arnold tongues for different unstable periodic orbits has confirmed that the domain of phase synchronization corresponds to the region where these tongues overlap (for details, see [Park *et al*, 1999]).

2.2 Imperfect phase synchronization as switching of locking ratios

The case of $r = 28$ offers a different picture. Let us discuss the relevant properties of Eqs.(3) at $E = 0$ since they, to a large extent, prescribe the way the system reacts to the periodic forcing. Here, the attracting set in the phase space is the well-known Lorenz attractor (Fig. 3a) which consists of two symmetric lobes and includes the saddle point at the origin along with the local component of its stable manifold. The trajectories which lie on this manifold never return onto the Poincaré plane; generic orbits in the course of evolution approach the stable manifold arbitrarily close, slow down and "hover" in the vicinity of the saddle point before departing along the one-dimensional unstable manifold; as a result, time intervals between two consecutive returns can be arbitrarily long. Although the events of this kind are rare (see Appendix F in [Sparrow, 1982]), their traces can be seen in the distribution of individual frequencies $\omega_{\rm i}$ for the unstable periodic orbits embedded into the chaotic attractor.

A procedure of denoting by 1 each orbit turn in the half-space $x > 0$, and, respectively, by 0 each turn in the half-space $x < 0$, endows each orbit with a symbolic binary label. For $1 < n \leq 27$, one can find in the Lorenz attractor the periodic orbit described by every (up to permutations) possible binary word of the length n [Sparrow, 1982].

The individual frequency of a periodic orbit is related to its geometry. The difference between the highest and the lowest values of $\omega_{\rm i}$ exceeds 10% of the mean frequency of the chaotic motion (Fig. 3b). For small and moderate ($\leq$25) values of n the highest value of $\omega_{\rm i}$ among the orbits of the length n is reached by the orbit of the type shown in Fig. 3c (here, for $n = 19$). Such orbit makes one turn in the half-space $x > 0$ (or, for its symmetric counterpart, in the space $x < 0$), approaches the saddle, leaves it along the unstable manifold and performs $n - 1$ turns in the half-space $x < 0$ (respectively, $x > 0$); correspondingly, its binary label is 100...0 (011...1). In a paradoxical way, a passage near the saddle, i.e. the slowing down in

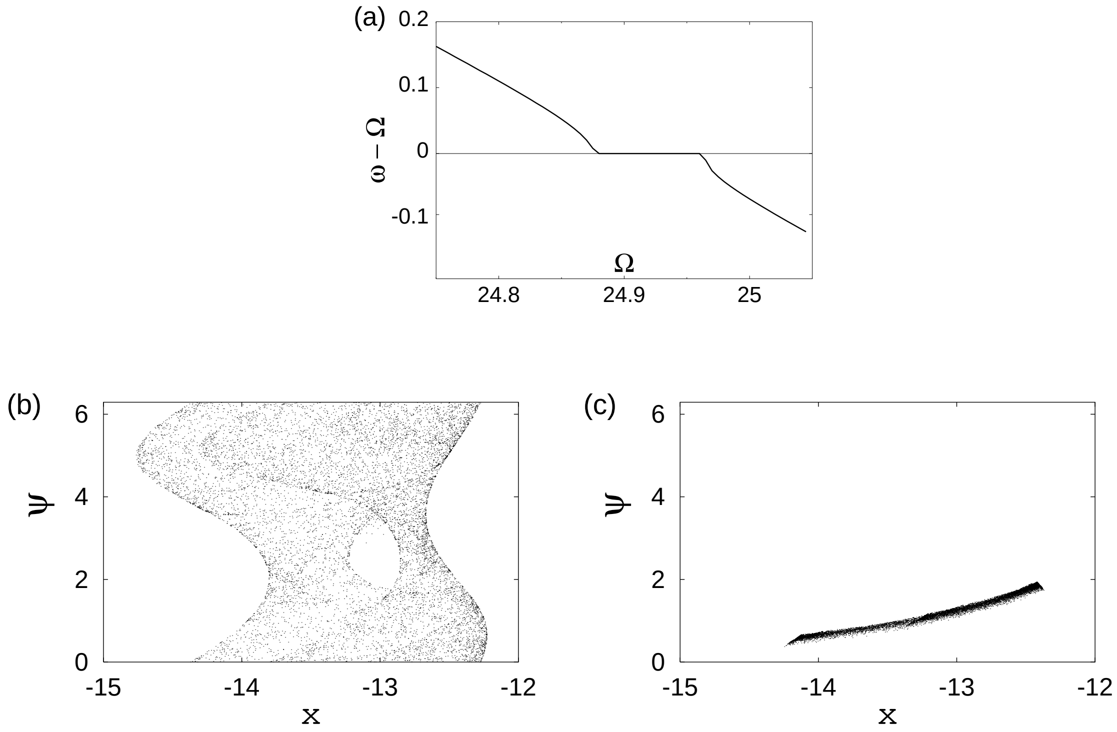

Figure 2: Phase synchronization at r=210:
(a) Difference between mean frequency of chaotic motion ω and driving frequency Ω for $E = 3$.
Attractors on the Poincaré plane for: (b) non-synchronized state ($\Omega = 24.8, E = 3$);
(c) phase-synchronized state ($\Omega = 24.94, E = 3$).

the phase space, leads ultimately not to the decrease but to the increase of the frequency. This owes to the particular geometry of the Lorenz attractor: after hovering near the saddle the trajectory is reinjected into the region adjacent to the saddle-foci points where the rotation rate is at fastest. Hence, the orbit consists of one very slow turn and $n-1$ rather fast ones; in the net effect the latter "overweight" the former, and the frequency averaged over the whole orbit is relatively high[2]. On the contrary, the orbit corresponding to the lowest value of $\omega_{\rm i}$ is located in the "middle" part of the attractor (Fig. 3d); it visits neither the region of slow motion near the saddle point nor the domains of fast rotations around the saddle-foci.

Although for all computed orbits the value of $\omega_{\rm i}$ is larger than 8, we expect that the band of individual frequencies should not be bounded from zero. In the range $24.06 < r \leq 33.6$ the values of r corresponding to secondary homoclinic bifurcations are dense (see e.g. [Sparrow, 1982]). Therefore, at every value of r from this interval (including, of course, $r = 28$) one should encounter the "newborn" unstable periodic solutions which are arbitrarily close to the homoclinic loops and whose period, thereby, is arbitrarily large. However we can argue that these orbits with exceptionally low individual frequencies are extremely unstable, which makes them not important from the point of view of global dynamics. The stability of a periodic orbit is characterized by its multipliers: eigenvalues of the linearized monodromy operator for the mapping on the Poincaré plane. Near the critical parameter value r_0 which corresponds to the homoclinic bifurcation, the mapping can be reduced to a discontinuous one-dimensional map [Sparrow, 1982];

[2]Naturally, in case of a passage very close to the saddle, the duration of this first turn can be arbitrarily high and cannot be balanced by subsequent rotations, so that also the averaged frequency would be arbitrarily small; as discussed below, this should take place only for orbits of rather high length n which do not seem to make a noticeable contribution to the dynamics.

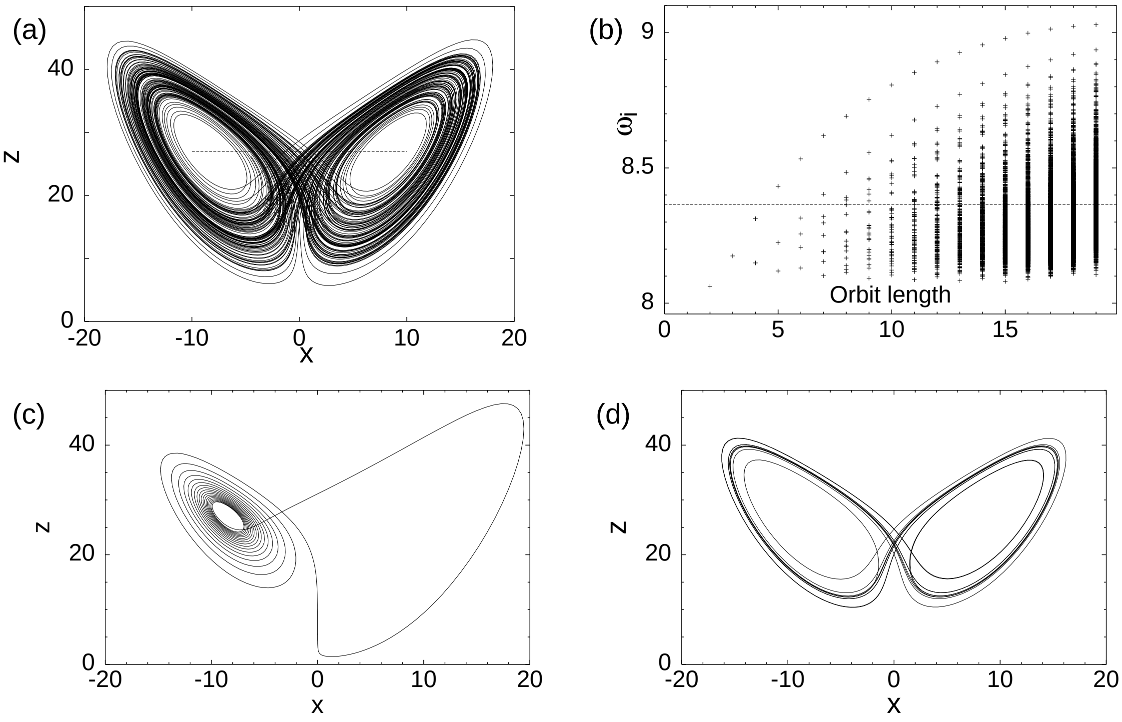

Figure 3: Autonomous Lorenz equations at r=28:
(a) projection of the attractor; solid line: Poincaré surface;
(b) individual frequencies of periodic orbits; dashed line: mean frequency of chaotic motion;
(c) periodic orbit of length 19 with the highest $\omega_{\rm i}$ ($\omega_{\rm i}$=9.029175);
(d) periodic orbit of length 19 with the lowest $\omega_{\rm i}$ ($\omega_{\rm i}$=8.105155).

analysis of this map shows that on approaching r_0 the largest characteristic multiplier behaves as $(r-r_0)^\nu$ with $\nu = 1+\lambda_u/\lambda_s$ being formed from the positive eigenvalue λ_u and the negative (the closest to zero of the two negative ones) eigenvalue λ_s of the saddle point at the origin. A direct calculation for $\sigma=10, b=8/3, r=28$ yields $\nu = (49-3\sqrt{1201})/16 \approx -3.44$. The contribution of each periodic orbit into the dynamics is inversely proportional to its characteristic multiplier [Grebogi *et al.*, 1987, Eckhardt & Ott, 1994]; this value rapidly diverges near r_0, which makes the significance of newborn orbits for the global behavior negligible. Besides, the length of such orbits must be noticeably larger than of those, presented in Fig. 3b: according to our numerical data, the first 27 letters in the symbolic label of the unstable manifold of the saddle point do not change within the interval $24.06 < r < 30$; this implies the absence of homoclinic orbits with a length shorter than 27 in this parameter range.

Now, let us introduce periodic forcing with a frequency close to the mean frequency of the chaotic autonomous motion, and check for phase synchronization. In Fig. 4a the difference between the frequency of the chaotic motion ω and the driving frequency Ω is plotted versus Ω for several different values of the forcing amplitude E. A synchronizing effect takes place, but it is definitely incomplete. Although each of the plotted curves shows a broad plateau, none of the plateaus is strictly horizontal (compare to Fig. 1c) and none of them lies at zero.

The inability to achieve perfect chaotic phase synchronization cannot be attributed to the weakness of the forcing term: further increase of E does not change the picture qualitatively, until, at $E > 20$, windows of stable periodic behavior appear. Location on the parameter plane of the main (corresponding to $1:1$ locking) Arnold tongues also provides no clue: as seen

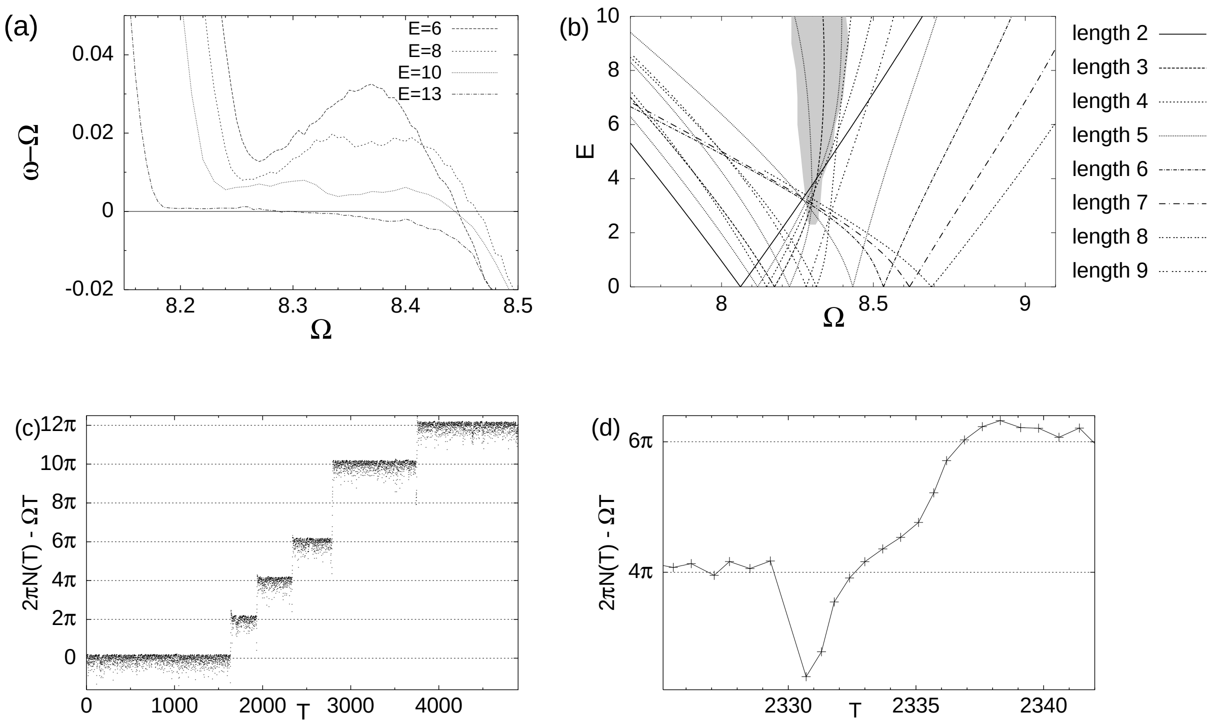

Figure 4: Imperfect phase synchronization at r=28:
(a) Difference between mean frequency of chaotic motion ω and driving frequency Ω;
(b) Arnold tongues on the parameter plane; shaded region: domain of synchronization;
(c) evolution of the difference between the phases ($\Omega = 8.3, E = 10$);
(d) blow-up for the neighborhood of the jump; crosses: intersections with Poincaré plane.

in Fig. 4b where the principal tongues [3] are plotted, the region of imperfect synchronization includes the domain where these Arnold tongues intersect and where, hence, one should expect matching between the phases like in Fig. 2a.

To understand the reasons for the imperfections in phase synchronization, it is helpful to follow the process in time and to focus on the temporal evolution of difference between the phase of the force and the phase of the system. The former is provided by Ωt; the latter can be recovered from Eq. (1). Let us pick up the parameter values corresponding to the left part of the plateau of approximate synchronization, set the equal starting values for the phases, and plot the difference between them as a function of time (Fig. 4c). The plot resembles a staircase built of long horizontal segments; minor deviations from the horizontal lines owe to the ill-definedness of the phase. The length of a horizontal segment usually corresponds to several thousands of turns of a chaotic orbit. The segments are interconnected by sharp phase jumps during which the difference between the phases rapidly increases by an increment of 2π (or, seldom, 4π). Along the first stair, the driving force and the driven system are roughly in-phase, in the second stair the phase of the system is 2π ahead, and so on. Thus, it appears that for most of the time the system remains synchronized with the force, and only the systematic phase jumps disturb from time to time the locking between phases.

A closer look shows that each jump upwards is preceded by a short decline downwards. During this decline, the phase of the force grows faster than the phase of the system; this

[3] It hardly makes sense to plot the tongues for all 224 orbits with length $l \leq 10$; we show the most typical ones, with the highest and the lowest individual frequencies.

means that at the beginning of each jump the motion of the system in the phase space is rather slow. Accordingly, the close-up of a typical jump (Fig. 4d) discloses that the jump is not instantaneous; its whole length occupies more than ten orbit turns. Comparison with other jumps shows their common feature: each of them corresponds to a segment of the orbit which, during l (l should be large enough) periods of external force, makes $l+1$ (or, seldom, $l+2$) returns onto the Poincaré surface. The difference between the turns on the plot is difficult to overlook: the first one requires the time interval which is much longer than the duration of the subsequent ones. This reminds the periodic orbits of the kind plotted in Fig. 3b: for such orbits the very slow turn which includes the passage near the saddle equilibrium, is followed by a sequence of short turns during which the system rapidly spirals around one of the saddle-focus points.

Let $\omega_{\rm min}$ and $\omega_{\rm max}$ denote the lower and the upper boundaries of the band of individual frequencies for the autonomous system. Consider in the forced system the torus originated from the particular autonomous periodic orbit of length l whose frequency has been close to $\omega_{\rm max}$. Let us choose the value of external frequency Ω in the lower part of this band. Then the torus may be locked by the external force not in the main ratio 1:1 (which would mean $\Omega=\omega_{\rm i}$) but in the ratio $(l-1):l$ (i.e. $\Omega=\omega_{\rm i}(l-1)/l$). Periodic orbits of length l on the surface of this torus close not after l but after $l-1$ periods of external force. During each passage near such orbit, the phase of chaotic trajectory would run 2π ahead with respect to the phase of the external force; this would result in the transition upwards, onto the next stair of Fig. 4c. To enable this, the periodic orbit should be long enough; the obvious rough estimate yields: $l>\omega_{\rm max}/(\omega_{\rm max}-\omega_{\rm min})$ which, in our case, means $l>9$.

Thus we see that the phase jumps are, in fact, time intervals in which the system is synchronized with the external force in the ratios different from 1:1. This conjecture is confirmed by the view of the Poincaré section of the attractor (Fig.5a). Here we show one chaotic trajectory and several unstable periodic orbits. Unlike the case of perfect synchronization (cf. Fig.2c), the attractor is not localized with regard to the variable Ψ. To elucidate the phase dynamics, we present the attractor together with two its identical replica which are shifted by 2π and 4π along Ψ. Most of the imaging points are located in the central part of the attractor; the rest is spread over the fine lateral structure which connects the attractor with its replica. In the course of evolution two types of phase dynamics alternate. The first type consists of long chaotic wandering over the central part of the attractor, among the tori locked in the ratio 1:1; here the system roughly remains in phase with the external phase. Dynamics of the second type begins in the vicinity of one of the tori locked in a different ratio; there the orbit drifts along the corresponding phase-stable orbit (these orbits for three of such tori are shown in the figure), gaining 2π in the phase variable.

In Fig.5b we focus on the action of the external force onto a particular periodic solution of the autonomous equations: one of the unstable periodic orbits of length 13. The plot presents the Arnold tongues which correspond to the main (1:1) and the 12:13 lockings for this orbit, respectively. The overlap of the tongues implies that in the parameter space of the forced equations there is a region with two phase-stable periodic orbits with *different* winding numbers which stem from the *same* periodic orbit of the autonomous case. Of course, such two closed orbits cannot coexist on the surface of a 2-torus; consequently, this torus, born from the corresponding closed curve of the autonomous equations and present at low values of the forcing amplitude, should be already destroyed for the amplitude values corresponding to the overlap. The absence of the smooth toroidal surface, however, seems not to hamper synchronization: what is needed, are the phase-stable periodic solutions. As seen in the plot, the overlap area on the parameter plane belongs to the region of imperfect phase synchronization. Sufficiently long segments of a chaotic trajectory should contain the passages near each of these two orbits.

During the passage near the orbit locked in the ratio 1:1, phases of the force and of the system grow "in parallel" whereas each passage near the orbit locked in the ratio 12:13 would result in the phase gain of 2π. Thus, imperfect phase synchronization appears to be a process in which different locking ratios alternate. In fact, it is hardly possible to check numerically whether *each* jump owes to the passage near an orbit of the described type; we can conclude that existence of these orbits is sufficient for imperfections in phase synchronization, but cannot exclude the action of other mechanisms.

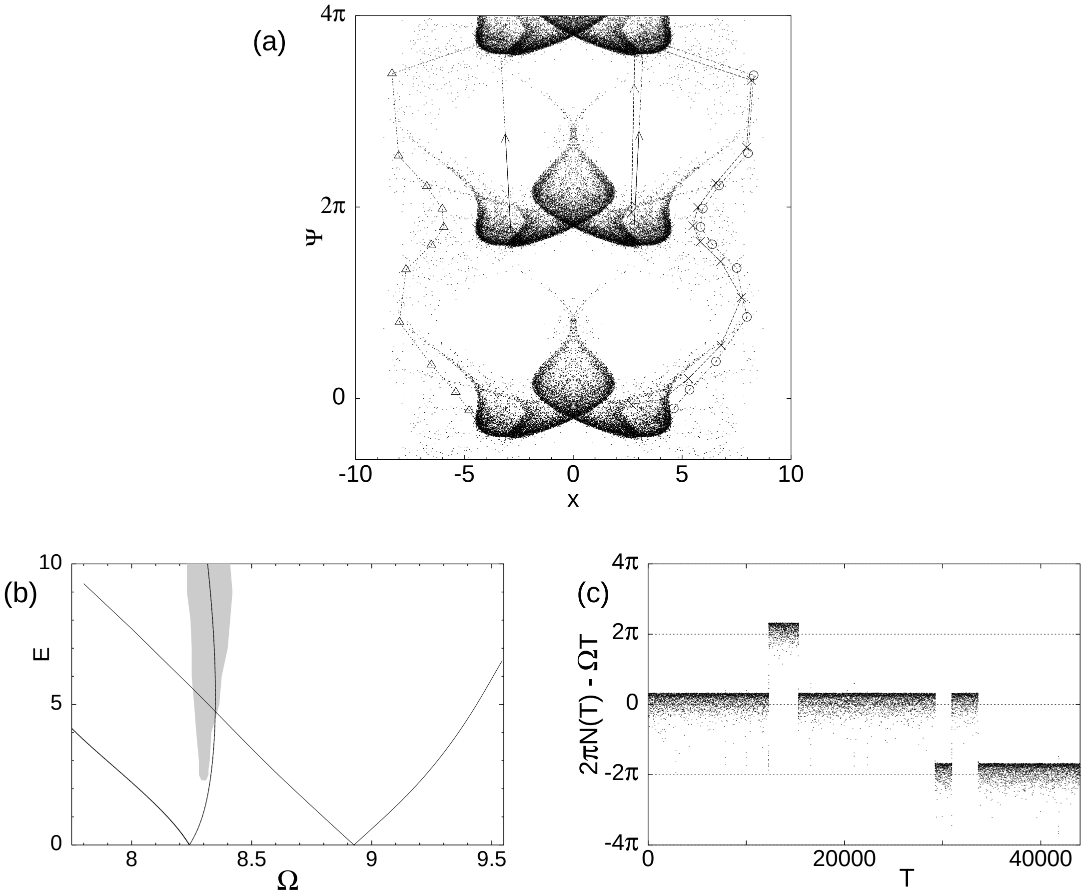

Figure 5: Alternation of locking ratios:
(a) periodic orbits embedded in the attractor on the Poincaré plane at $E = 10, \Omega = 8.3$. Crosses, circles, triangles: periodic orbits, locked in ratios 12:13, 13:14 and 14:15, respectively; arrows show the direction of motion. Dots: chaotic trajectory.
(b) Main locking region (right) and the region of locking 12 : 13 (left) for the periodic orbit of length 13. Gray domain: region of imperfect phase synchronization.
(c) Jumps upwards and downwards in the evolution of phase difference. $E = 14$; $\Omega = 8.25$.

The situation in the right part of the synchronization plateaus is different; here, in the temporal evolution of the phase difference, one observes the jumps both upwards and downwards (Fig.5c). Altogether, the scenario which evolves during the increase of Ω across the region of imperfect phase synchronization, can be described in the following way. Although at low values of Ω some of the tori are synchronized in the ratios $m : l$ where l is the length of the original autonomous periodic orbit and m is noticeably smaller than l, the rare passages near these lockings are statistically negligible and do not produce visible changes in the general picture of non-synchronized motion. On increasing Ω, we enter the parameter region in which most of the tori are locked in the ratio 1:1, while some other (originated from the longer autonomous periodic orbits with high individual frequencies ω_i) are locked in the ratios$(l-1):l$; this is the left part of the region of imperfect phase synchronization. One can expect that the shorter orbits produce a bigger contribution into the dynamics [Hunt & Ott, 1996]; therefore, for most of the time the chaotic trajectories remain near the "correctly" locked tori and the phase of the system does not depart from the phase of the force. During each of relatively rare visits into the neighborhood of one of the tori locked in the ratio $(l-1):l$ the phase difference grows by a 2π increment[4]. Formally, we can write $\omega = \Gamma\Omega$, with $\Gamma = \Gamma(\Omega)$ being a kind of a global "winding number". Each torus contributes to the global value of Γ; due to countable number of singularities on the borders of Arnold tongues, the function $\Gamma(\Omega)$ is, in general, not differentiable. In the described domain the individual winding numbers ω_i/Ω equal 1 for most of the tori, whereas for the tori locked outside of the main Arnold tongue these numbers equal $l/(l-k), k = 1, 2, \ldots$ i.e. are larger than 1. As a result, the global Γ is slightly larger than 1. Re-writing $\omega - \Omega$ as $(\Gamma - 1)\Omega$ we see that in this parameter domain the slope of the synchronization plateau is (piecewise) positive. With increase of Ω we cross one-by-one the right borders of the Arnold tongues corresponding to the described lockings. Although most of the tori remains locked, chaotic trajectories visit from time to time the vicinities of non-synchronized tori. During such passages the difference between the phases decreases (cf. the transitions downwards in Fig.5c). Further increase of Ω unlocks further tori, and the slope of synchronization plateau becomes negative. Finally, we reach the stage at which most of the tori originated from short orbits are out of the 1:1 locking; this marks the end of approximate phase synchronization.

3 Periodically forced Shimizu-Morioka equations

As an example of a chaotic system which in the autonomous case is close to formation of homoclinic orbits of short length, we take the Shimizu-Morioka equations [Shimizu & Morioka, 1980] perturbed by external periodic force:

$$\begin{aligned} \dot{x} &= \kappa x - \lambda y - yz \\ \dot{y} &= x \\ \dot{z} &= y^2 - z + E\cos\Omega t \end{aligned} \tag{4}$$

The autonomous ($E = 0$) equations (4) were proposed in [Shimizu & Morioka, 1980] as a model which imitates the dynamics of the Lorenz system at high values of r. The physical relevance of these equations was discussed in [Rucklidge, 1992]. They were shown to be a variant of the normal form which governs the dynamics near the intersection of the oscillatory and monotonic instabilities for the heated horizontal layer of the conductive fluid put into a vertical magnetic field.

The bifurcation sequences on the 2-parameter plane of the autonomous Shimizu-Morioka equations were explored in [Shilnikov, 1993, Rucklidge, 1993], where, in particular, the loci in the parameter space of primary and secondary homoclinic bifurcations of the saddle point at the origin were determined; invariance of equations with respect to the change of sign $\{{x \atop y}\} \leftrightarrow \{{-x \atop -y}\}$ turns such bifurcations into homoclinic explosions [Sparrow, 1982] at which the whole countable sets of periodic orbits are born or eliminated.

For our numerical experiments we need the parameter values which ensure the existence of a chaotic attractor in the autonomous system. By choosing in the autonomous system $\kappa = -2$ and

[4]Apparently the even more seldom jumps of 4π are due to the passage near the orbits locked in the ratio $(l-2):l$. To enable this, l should exceed $2\omega_{\max}/(\omega_{\max} - \omega_{\min})$ i.e., for our equations, $l \geq 20$. In fact, we were able to identify within the attractor periodic orbits locked in the ratio 18:20 [Zaks *et al.*, 1999].

varying λ between $-6\frac{1}{2}$ and $-5\frac{1}{2}$, we detect the homoclinic orbit of length 3 at $\lambda = -5.5415\ldots$, orbit of length 4 at $\lambda = -6.1628\ldots$, orbits of length 5 at $-5.7816\ldots$ and $-6.3982\ldots$, orbits of length 6 at $-6.0489\ldots, -6.2607\ldots$ and $-6.4929\ldots$, etc. Below we fix the values $\kappa = -2$ and $\lambda = -6$; projection of the corresponding chaotic attractor in the autonomous system is plotted in Fig. 6.

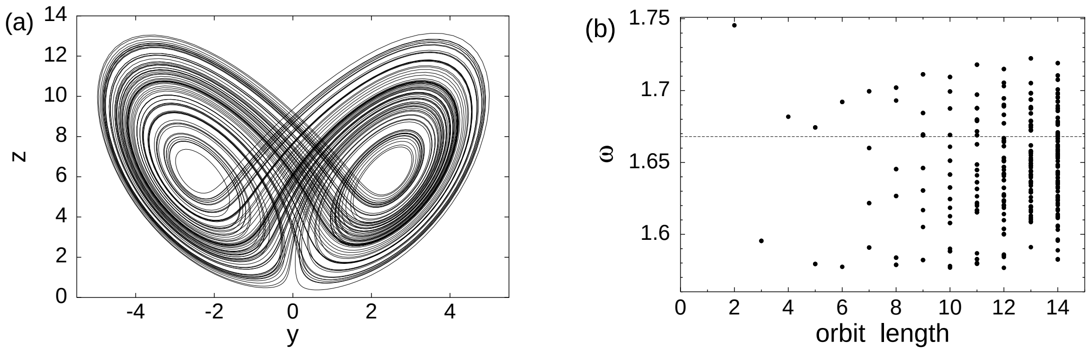

Figure 6: Autonomous Shimizu-Morioka equations at $\kappa = -2, \lambda = -6$:
(a) projection of the attractor; (b) individual frequencies of periodic orbits.

In the sense of symbolic dynamics, the chaos of the Shimizu-Morioka equations at $\kappa = -2, \lambda = -6$ is "poorer" than the chaos of the Lorenz equations at $r = 28$: the number of periodic orbits is distinctly lower, many of the binary labels are non-admissible. This has to do with the fact, that for the attractors of the Lorenz type the symbolic dynamics is at richest at their birth, whereas the secondary homoclinic explosions (amid which lies our chosen parameter set) only "dismantle" the attractor, by destroying the whole countable subsets of periodic orbits [Sparrow, 1982]. As a result, the distribution of individual frequencies for the periodic orbits in the autonomous system, as shown in Fig. 6b differs from the similar distribution in the Lorenz equations. The orbits with symbolic labels 100...0, with their slow passage near the saddle and subsequent fast rotations, are missing; geometrically, this means that the lobes of the attractor are well separated from the saddle-focus points, and do not include regions of fast rotations.

We study synchronization properties of Eqs.(4) in the same way as for the Lorenz system, fixing the driving amplitude E and searching for the plateaus in the dependencies of $\omega - \Omega$ on Ω. Typical results for several values of E are presented in Fig.7a. The plateaus are located close to the mean frequency of the chaotic motion $\omega = 1.668$; similarly to the case of the forced Lorenz system, none of them is horizontal. Unlike the case of the Lorenz system, where at least some parts of the plateau lie above zero, here all the plateaus are invariably located in the negative half-plane. This means that the phase jumps are uni-directional and cause the phase lag of the driven system with respect to the driving force. Further, the non-monotonicity of $\omega - \Omega$ within the plateaus, typical for the Lorenz case (cf. Fig. 4a), is absent: the slope of the plateaus in the forced Shimizu-Morioka equations is negative.

These differences from the familiar picture of imperfect phase synchronization can be interpreted in terms of unstable periodic orbits, and a prompt comes again from the time growth of the difference between the phases (Fig.7b). As we can see in Fig.7c, a jump starts with the long orbit turn in which the slowdown is apparently caused by the passage close to the saddle point. Since after such passage the trajectory is reinjected into the region of rotations with moderate rate, the phase loss is not compensated, and the system eventually settles down on the stair located 2π lower. Such behavior should occur in the neighborhoods of unstable tori on which the periodic orbits are locked in the $(l+1):l$ ratios, i.e. consist of l turns and close

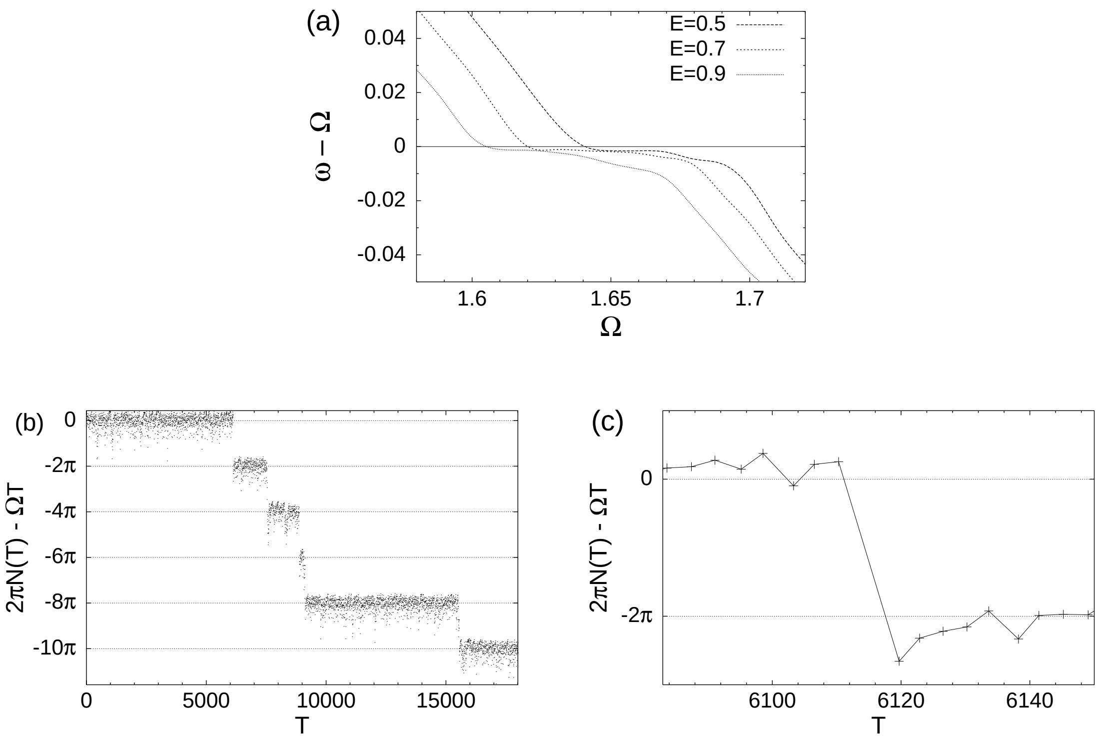

Figure 7: Imperfect phase synchronization in Eq. (3) at $\kappa = -2$, $\lambda = -6$:
(a) difference between mean frequency of chaotic motion ω and driving frequency Ω;
(b) evolution of difference between phases for E=0.7, Ω=1.64;
(c) neighborhood of a phase jump; crosses: intersections with Poincaré plane.

after $l+1$ periods of the external force. These tori originate from the orbits of the autonomous system whose individual frequencies in the distribution of Fig. 6 lie close to the minimal value $\omega_{\rm min}$. The requirement that the locked frequency $(l+1)\omega_{\rm i}/l$ would still be smaller than $\omega_{\rm max}$ provides the estimate for the length l: $l \leq \omega_{\rm min}/(\omega_{\rm max}-\omega_{\rm min})$ which, in our case, means $l \geq 10$. Individual winding numbers $l/(l+1)$ for such orbits are smaller than one; due to their contribution, the global winding number Γ is also slightly smaller than one. Hence, the prefactor in the expression $(\Gamma-1)\Omega$ is weakly negative; this explains the negative slope of the synchronization plateaus when $\omega-\Omega=(\Gamma-1)\Omega$ is plotted against Ω.

In Fig.8 we present the location of Arnold tongues on the parameter plane, along with the domain of imperfect phase synchronization. The main Arnold tongues corresponding to the 1:1 locking for the periodic orbits of length $l \leq 8$, are plotted in Fig.8a. As can be seen in Fig.8b, for certain orbits (here, for $l=8$) not the main locking $1:1$ but the locking $(l+1):l$ appears to be of importance for phase synchronization.

The remarkable property of the bifurcation diagram in Fig. 8 is the unconventional shape of the Arnold tongues: for some of them the slope of the left border on the parameter plane at low values of the driving frequency Ω is unusually small. It appears that such borders tend to horizontal asymptotes; numerically, we encountered problems in continuation of these borders further into the domain of low frequencies. The phase portrait of the corresponding marginal periodic solution includes segments in which the trajectory passes relatively close to the origin, reminding of homoclinic orbits in the autonomous system. The following argument shows that such orbits may be of certain relevance. The periodically forced Eqs. (4) have an apparent

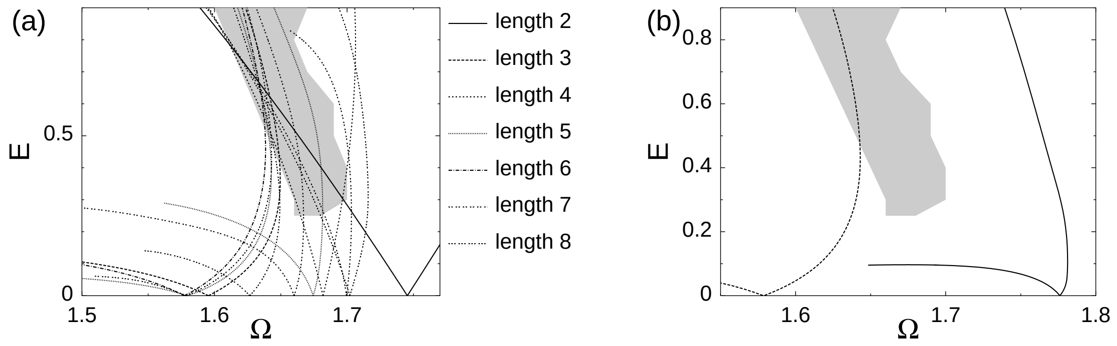

Figure 8: Locking regions for the forced Shimizu-Morioka equations:
(a) main Arnold tongues; shaded region: domain of imperfect phase synchronization;
(b) Arnold tongues for the orbit of length 8: locking ratio 1:1 (left) and locking ratio 9:8 (right).

periodic solution:

$$x_p(y) = y_p(t) = 0; \quad z_p(t) = \frac{E}{\sqrt{\Omega^2+1}} \cos(\Omega t - \arctan \Omega). \tag{5}$$

Let us shift the time by $\Omega^{-1} \arctan \Omega$ and rewrite the equations in the "co-rotating" reference frame by introducing the variable $\tilde{z} \equiv z - z_p(t)$:

$$\begin{aligned} \dot{x} &= y \\ \dot{y} &= \kappa x - (\lambda + \frac{E}{\sqrt{\Omega^2+1}} \cos \Omega t) y - y \tilde{z} \\ \dot{\tilde{z}} &= x^2 - \tilde{z} \end{aligned} \tag{6}$$

Thus viewed, periodic forcing turns into the periodic modulation of the parameter λ. Assuming the values $E \approx 1/2$ and $\Omega \approx 1.65$ which correspond to the states of imperfect phase synchronization, we see that the "instantaneous" value of κ oscillates between 5.75 and 6.25; in the autonomous case (see the data above) this would correspond to the passage through several homoclinic bifurcations which involve trajectories of short length[5].

To explain the unusual shape of the locking regions, we consider the general case when the weak harmonic forcing acts onto a system, which in the absence of perturbation possesses a periodic orbit close to the unstable manifold of the saddle point. This situation was described in [Afraimovich & Shilnikov, 1991]; unlike that work where the frequency of the forcing was not explicitly accounted for, we treat it as an independent parameter.

In the frame of "co-rotating" coordinates $x, y, \tilde{z}$ the equations have an equilibrium point at the origin $x = y = \tilde{z} = 0$. The local unstable manifold of this point is tangent to the xy plane whereas the "leading" (corresponding to the closest to zero of two negative eigenvalues) direction of the local stable manifold is tangent to the $\tilde{z}$-axis . The usual formalism, widely employed in the context of homoclinic bifurcations, is based on the reduction of the flow to a mapping [Shilnikov, 1968]. For this purpose consider two planes close to the origin: the Poincaré plane p which is orthogonal to the leading direction of the stable manifold and lies at a distance $\tilde{z}_p$ from the equilibrium, and the auxiliary plane q which is orthogonal to the unstable manifold (Fig. 9). The trajectories can be decomposed into the local (close to the "equilibrium") and

[5]A similar procedure for the forced Lorenz equations from the preceding section would provide the "instantaneous" values of r between 26 and 30; as mentioned above, although bifurcational values corresponding to homoclinic explosions are dense in this interval, the orbits with the length $l \leq 27$ are not concerned.

global segments; accordingly, the Poincaré mapping induced by the flow can be viewed as a subsequent composition of the "local" map from p into q and the "global" map from q back into p. Below we mark the coordinates of points on these planes with respective indices.

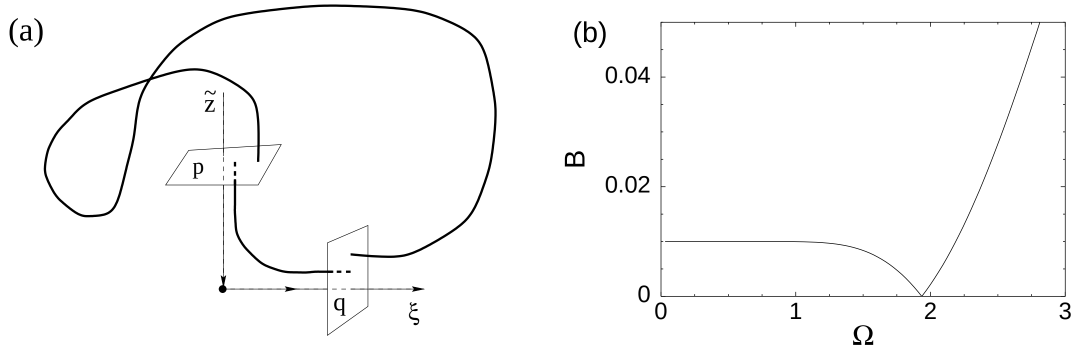

Figure 9: Locking regions near homoclinicity:
(a) derivation of the return mapping;
(b) shape of the tongue according to Eq.(12); λ_u=3, λ_s=-2, $n = \tau_{qp} = A = \tilde{z}_p = \xi_q$=1, μ=0.01.

Let the unstable manifold be parameterized by means of the coordinate ξ so that the plane q is located at ξ_q. As a coordinate characterizing the external forcing, it is convenient to take the phase Ψ of the force. The motion from p to q can be considered as governed by the linearized equations:

$$\dot{\xi} = \lambda_u \xi, \qquad \dot{\tilde{z}} = \lambda_s \tilde{z}, \qquad \dot{\Psi} = \Omega \tag{7}$$

with λ_u being the only positive eigenvalue and λ_s the closest to zero negative eigenvalue of the saddle point (the time-dependent term in the first equation has been neglected due to smallness of the amplitude E). Therefore the mapping from p into q is:

$$\begin{aligned} \tilde{z}_q &= \tilde{z}_p \exp(\lambda_s \tau_{pq}) = \tilde{z}_p \left(\frac{\xi_p}{\xi_q}\right)^{-\lambda_s/\lambda_u} \\ \Psi_q &= \Psi_p + \Omega \tau_{pq} \end{aligned} \tag{8}$$

where $\tau_{pq} = \lambda_u^{-1} \log \xi_q/\xi_p$ is the time of passage from p to q.

Since both $\tilde{z}_q$ and the amplitude of the forcing are assumed to be small, the mapping from q to p can be in the lowest order written as

$$\begin{aligned} \hat{\xi}_p &= -\mu + A\tilde{z}_q + B \sin \Psi_q + \text{h.o.t.} \\ \hat{\Psi}_p &= \Psi_q + \Omega \tau_{qp} \end{aligned} \tag{9}$$

where B is proportional to the forcing amplitude E and τ_{qp} is the time of passage from q to p along the global segment of the trajectory; in the lowest order, the value of τ_{qp} can be treated as a constant. The parameter μ characterizes in the autonomous system the distance from the bifurcation: in the absence of forcing, $\mu = 0$ would correspond to the formation of the homoclinic orbit whose breakup would create a periodic solution. If the inequality $\lambda_u + \lambda_s > 0$ holds (as is the case of the autonomous Eqs.(4) at $\kappa = -2$, $\lambda = -6$) this periodic solution exists for $\mu > 0$ and is unstable [Shilnikov, 1968].

Composition of the maps (8) and (9) yields the lowest order of the mapping of p into p:

$$\begin{aligned} \hat{\xi}_p &= -\mu + A\tilde{z}_p \left(\frac{\xi_p}{\xi_q}\right)^{-\lambda_s/\lambda_u} + B \sin(\Psi_p + \Omega \tau_{pq}) \\ \hat{\Psi}_p &= \Psi_p + \Omega(\tau_{pq} + \tau_{qp}) \end{aligned} \tag{10}$$

The orbit of the continuous system which returns onto the plane p in the vicinity of the saddle point after n periods of external force is, in terms of the combined mapping, described by the fixed point $\hat{\xi}_p = \xi_p, \quad \hat{\Psi}_p = \Psi_p + 2\pi n$; explicit equations for this fixed point are:

$$\begin{aligned} \xi_p &= -\mu + A\tilde{z}_p \left(\frac{\xi_p}{\xi_q}\right)^{-\lambda_s/\lambda_u} + B\sin(\Psi_p + \frac{\Omega}{\lambda_u}\log\frac{\xi_q}{\xi_p}) \\ 2\pi n &= \Omega\tau_{qp} + \frac{\Omega}{\lambda_u}\log\frac{\xi_q}{\xi_p} \end{aligned} \tag{11}$$

Existence of the fixed-point is ensured by the condition of solvability for eqs. (11):

$$\pm B = \mu + \xi_q \mathrm{e}^{\lambda_u(\tau_{qp} - 2\pi n/\Omega)} - A\tilde{z}_p\xi_q \mathrm{e}^{-\lambda_s(\tau_{qp} - 2\pi n/\Omega)}\,; \tag{12}$$

this provides two branches of the saddle-node bifurcation which delineate the locking region. Irrespective of the values of the other parameters (recall that $\lambda_u + \lambda_s > 0$, $n \geq 1$, whilst the values of $\tilde{z}_p$, ξ_q and, hence, A are scalable) we obtain on the plane of parameters Ω and B the "infinitely flat" horizontal asymptote for the border of this region at $\Omega \to 0$. The typical shape of the locking region described by Eq. (12) is presented in Fig.9b.

4 Imperfect phase synchronization in the forced Ginzburg-Landau model

Another example of imperfect phase synchronization is delivered by the periodically forced low-dimensional model of the weakly dissipative two-dimensional complex Ginzburg-Landau equation. Starting from this equation (see e.g. [Cross & Hohenberg, 1993]) in the form

$$\mathrm{i}\frac{\partial u}{\partial t} + \nabla^2 u + 2|u|^2 u = \mathrm{i}(\varepsilon_1 u - \varepsilon_2 |u|^2 u + \varepsilon_3 \nabla^2 u), \tag{13}$$

one can represent the complex variable u in the trigonometric form: $u(x, y, t) = a \exp i\phi$ where a and ϕ are real, expand a into the trigonometric series of the perturbation wavenumber q_0: $a(x, y, t) = a_0 + \sum_{m,n} b_{mn}(t) \cos q_0 mx \cos q_0 ny$ and, finally, arrive at the set of ODEs for the coefficients b_{mn}. It can be shown that in the limit of small $\varepsilon_{1,2,3}$ the active oscillating modes near the boundary of the modulational instability are governed by the 5-dimensional set of equations which on the invariant subspace $b_{01} = b_{10}$ can be further reduced to a system of the 3-rd order with a cubic nonlinearity: (see [Zaks *et al.*, 1996] for the details of the derivation):

$$\begin{aligned} \ddot{X} + 2(1+4A)\dot{X} &= (16K - 8A - 16A^2 + 32Y + 24X^2)X \\ \dot{Y} + \dot{X}X &= -2Y - (5+4A)X^2, \end{aligned} \tag{14}$$

where the variables X and Y are the rescaled b_{10} and b_{00}, respectively, and the parameters A and K can be expressed through the original coefficients $\varepsilon_{1,2,3}$ of the Ginzburg-Landau equation. The bifurcation scenarios for Eq.(14) were described in [Zaks *et al.*, 1996]; it was shown that the routes to chaos lead through the formation of homoclinic orbits to the saddle equilibrium. Correspondingly, the return times on the attractor are unbounded. For our current purpose, we fix the values $A = 1, K = 4.4$ under which the dynamics of (14) is chaotic, and add to the last of the equations the periodic forcing $E\cos\Omega t$.

As recognizable in Fig. 10, the mechanism of phase synchronization in this case reproduces the basic features of the similar process in the periodically driven Shimizu-Morioka system.

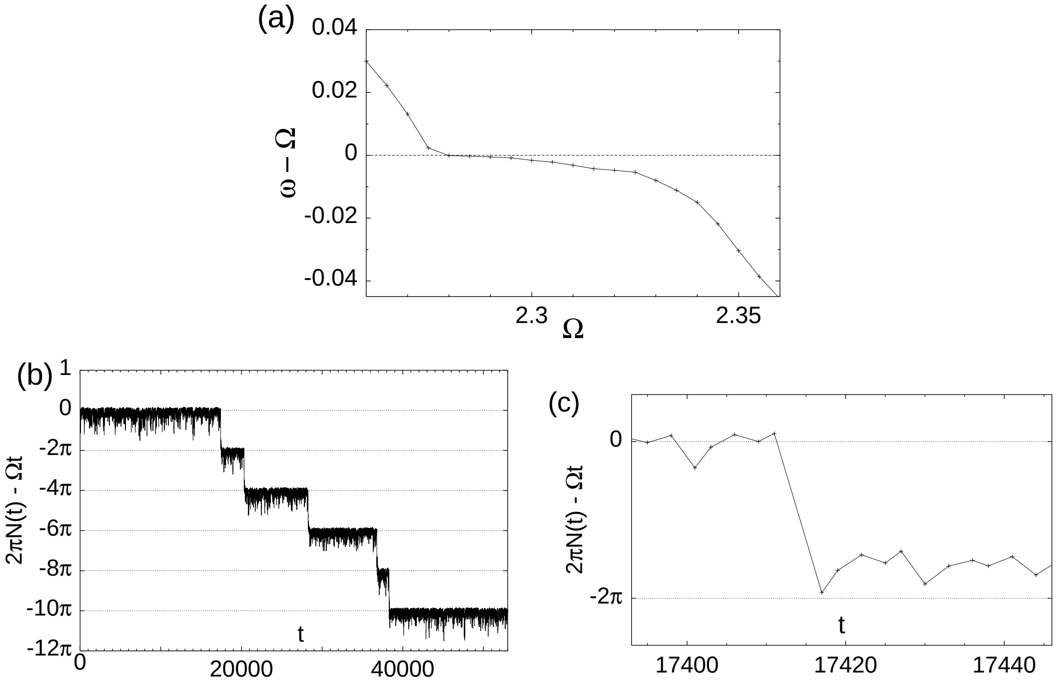

Figure 10: Synchronization in the forced Eqs.(14) at $E = 0.03$:
(a) plateau of imperfect phase synchronization;
(b) time evolution of the phase difference, $\Omega = 2.285$;
(c) neighborhood of a typical phase jump; crosses: intersections with Poincaré plane.

The appropriate Poincaré plane for the computations is chosen at the fixed value $Y = (5 + 4A)(2K - A - A^2)/(16A + 14)$. The non-flat plateau in Fig. 10a indicates to the imperfect character of synchronization. The everywhere negative slope of this plateau implies that the chaotic trajectory, while keeping in pace with the external force for most of the time, sometimes lags behind. The latter effect should be attributed to sporadic switchings from the locking ratio 1 : 1 to the ratios which are larger than 1, caused by the passage near the corresponding unstable tori in the phase space. The typical evolution of the difference between the individual phases of the driving force and the chaotic system is presented in Fig. 10b; it can be seen that the relatively long "stairs" are interrupted by short transitions downwards. Zooming in the neighborhood of a transition (Fig. 10c) we recover the familiar picture (cf.Fig.7c): the process starts with a long interval between two returns onto the secant plane, and continues through several shorter ones. We can identify the initial interval as the passage of the orbit through the zone of the slow motion around the origin.

5 Discussion

We have described here typical features of systems exhibiting imperfect phase synchronization. Our results allow to expect that this kind of synchronization can occur in many periodically forced chaotic systems. Unstable steady states play important dynamical role in a variety of problems of fluid mechanics, nonlinear optics, physical chemistry, etc.; accordingly, unstable fixed points should be present in the appertaining finite-dimensional models of these problems. Often, unlike our examples of pure saddle-like dynamics, these fixed points are of the saddle-focus type; dynamically, such systems are more complex, and the adequate description of synchronization for this situation is still missing.

Differences between perfect and imperfect types of phase synchronization should be visible in the structure of the parameter space as well; this is caused by the differences in the nature of corresponding attractors. Perfect phase synchronization can be encountered when the periodic force acts on "coherent" chaotic attractors with weak variations of return time. Such attractors can arise e.g. as a result of the period-doubling sequence. As long as autonomous systems are adequately modeled by unimodal mappings, domains of chaotic behavior in their parameter space are interspersed with dense windows of periodic dynamics [Graczyk & Swiatek, 1997]. For this reason, one should expect to find in the parameter space of *forced* systems similar windows of synchronized periodic dynamics. If, among the periodic solutions of an autonomous system, there is a stable one, it may be not necessary to enforce the locking of the other periodic orbit in order to synchronize the motion: to lock just one attracting torus may prove sufficient, and this can be achieved with arbitrarily small amplitude of forcing. Imperfect chaotic synchronization, on the other hand, appears to be robust: dynamics of the Lorenz type is persistent, and in order to arrive at stable periodic motions or invoke other qualitative changes in it, one would require noticeably high values for the amplitude of external force.

Periodic orbits which stand behind the mechanism of imperfections, occupy a certain intermediate position: in some sense, they are close to homoclinic orbits; in some sense, they remain far enough from them. Closeness is necessary in order to display a sufficient slowdown. However, if these orbits would be too close to homoclinicity, they would be highly unstable and play no noticeable role in dynamics. As a parameter, characterizing the distance from homoclinicity, one might use the largest Lyapunov exponent of the periodic orbit per orbit turn: on approaching homoclinic trajectory, this characteristics should diverge, but for the dynamically relevant orbits it should remain moderate.

Our last remark concerns the applicability of results to experimental data of physical, geophysical and medical origin. In the real world it is hardly possible to separate purely deterministic dynamics from noisy and often non-stationary background. Parameter drift, taken alone, can change the intrinsic frequencies; apparently, this is one of the mechanisms which stands behind the switching of locking ratios observed in natural systems, e.g. in the human cardiorespiratory data [Schäfer *et al.*, 1998, Schäfer *et al.*, 1999]. The appropriate theoretical framework for these phenomena, which should embrace both the dynamical and the stochastic aspects, is still to be elaborated.

Acknowledgement. We are grateful to M. Rosenblum, A. Pikovsky and D. Turaev for stimulating discussions. The research of M. Z. was supported by an MPG grant and SFB "Komplexe Nichtlineare Prozesse". E.-H.P. acknowledges the support of the Graduiertenförderungsprogram Landes Brandenburg.

References

Afraimovich, V. S. & Shilnikov, L. P. [1991] "Invariant two-dimensional tori, their breakdown and stochasticity", *Amer. Math. Soc. Transl.* **149**, 201–212.

Cross, M. C. & Hohenberg, P. C. [1993] "Pattern formation outside of equilibrium", *Rev. Mod. Phys.* **65**, 851–1112.

Cvitanović, P. [1991] "Periodic orbits as the skeleton of classical and quantum chaos", *Physica D* **51**, 138–151.

Eckhardt, B., Ott, G. [1994] "Periodic orbit analysis of the Lorenz attractor", *Z. Phys. B* **93**, 259–266.

Fujisaka, H. & Yamada, T. [1983] "Stability theory of synchronized motion in coupled-oscillator systems", *Prog. Theor. Phys.* **69**, 32.

Gabor, D. [1946] "Theory of communication", *J. IEE London* **93**, 429–457.

Graczyk, J. & Swiatek, G. [1997] "Generic hyperbolicity in the logistic family", *Annals of Mathematics* **146**, 1–52.

Grebogi, C. *et al.* [1987] "Unstable periodic orbits and the dimension of chaotic attractors", *Phys. Rev. A* **36**, 3522–3524.

Hunt, B. R. & Ott, E. [1996] "Optimal periodic orbits of chaotic systems", Phys. Rev. Lett. **76**, 2254–2257 (1996).

Kocarev, L. & Parlitz, U. [1996] "Generalized synchronization, predictability, and equivalence of unidirectionally coupled dynamical systems", *Phys. Rev. Lett.* **76**, 1816–1819.

Lorenz, E. N. [1963] "Deterministic nonperiodic flow", *J. Atmos. Sci.* **20**, 130–141.

Park, E.-H. *et al.* [1999] "Phase synchronization in the forced Lorenz system", *Phys. Rev. E* **60**, 6627-6638.

Pecora, L. M. & Caroll, T. L. [1990] "Synchronization in chaotic systems", *Phys. Rev. Lett.* **64**, 821–824.

Pikovsky, A. S. [1984] "On the interaction of strange attractors", *Z. Phys. B* **55**, 149–154.

Pikovsky, A. S. *et al.* [1997a] "Attractor-repeller collision and eyelet intermittency at the transition to phase synchronization", *Phys. Rev. Lett.* **79**, 47–50.

Pikovsky, A. S. *et al.* [1997b] "Phase synchronization of chaotic oscillations in terms of periodic orbits", *CHAOS* **7**, 680–687.

Pikovsky, A. S. *et al.* [1997c] "Phase synchronization of chaotic oscillators by external driving", *Physica D* **104**, 219–238.

Pikovsky, A. S. *et al.* [2000] "Phase Synchronization in Regular and Chaotic Systems: a Tutorial" *Int. J. of Bifurcation and Chaos*, this issue.

Rosa, E. R. *et al.* [1998] "Transition to phase synchronization of chaos", *Phys. Rev. Lett.* **80**, 1642–1645.

Rosenblum, M. G. et al. [1996] "Phase synchronization of chaotic oscillators", *Phys. Rev Lett.* **76**, 1804–1807 (1996).

Rucklidge, A. M. [1992] "Chaos in models of double convection", *J. Fluid Mech.* **237**, 209–229.

Rucklidge, A. M. [1993] "Chaos in a low-order model of magnetoconvection", *Physica D* **62**, 323–337.

Rulkov, N. F. *et al.* [1995] "Generalized synchronization of chaos in directionally coupled chaotic systems", *Phys. Rev. E* **51**, 980–994.

Rulkov, N. F. [1996] "Images of synchronized chaos: experiments with circuits", *CHAOS* **6** 262–279.

Schäfer, C. *et al.* [1998] "Heartbeat synchronized with ventilation", *Nature* **392**, 239–240.

Schäfer, C. *et al.* [1999] "Synchronization in the Human Cardiorespiratory System", *Physical Review E*, **60**, 857–870, 1999.

Shilnikov, L. P. [1968] "On the generation of a periodic motion from a trajectory doubly asymptotic to an equilibrium state of saddle type", *Math. USSR-Sb.* **6**, 428–438.

Shilnikov, A. L., "On bifurcations of the Lorenz attractor in the Shimizu-Morioka model", *Physica D* **62**, 338–346.

Shimizu, T. & Morioka, N. [1980] On the bifurcation of a symmetric limit cycle to an asymmetric one in a simple model, *Phys. Lett. A* **76**, 201–204.

Sparrow, C. [1982] *"The Lorenz equations : Bifurcations, chaos, and strange attractors"* (Springer-Verlag, NY).

Zaks, M., Nepomnyashchy, A., Malomed, B. [1996] "Onset of chaos in the weakly dissipative two-dimensional complex Ginzburg-Landau equation", *Physica Scripta* **T67**, 143–147.

Zaks, M. *et al.* [1999] "Alternating locking ratios in imperfect phase synchronization", *Phys. Rev. Lett.* **82**, 4228–4231.